High Pressure Research
Vol. 29, No. 4, December 2009, 665–670

Taylor & Francis
Taylor & Francis Group

Compressibility of insulin amyloid fibrils determined by X-ray diffraction in a diamond anvil cell

Filip Meersman[a,b]*, Raúl Quesada Cabrera[b], Paul F. McMillan[b] and Vladimir Dmitriev[c]

[a]*Department of Chemistry, Katholieke Universiteit Leuven, Leuven B-3001, Belgium;* [b]*Department of Chemistry, University College London, London WC1H 0AJ, UK;* [c]*Swiss-Norwegian Beamlines, ESRF, Grenoble F-38043, France*

(*Received 15 September 2009; final version received 21 September 2009*)

Amyloid fibrils are fibrous structures that originate from the self-assembly of polypeptides. Their formation is linked to debilitating diseases associated with protein misfolding, including Alzheimer's disease and type-II diabetes. In recent years, it has been suggested that such protein and polypeptide fibrils might provide useful novel nanomaterials. Here, we present the results of a study on the high pressure stability and compressibility of mature amyloid fibrils of insulin by synchrotron X-ray diffraction in a diamond anvil cell. The diffraction results allow a direct estimation of the elastic modulus and the corresponding compression of the cross-β structure along the fiber axis. The average hydrogen bond compressibility is comparable to that in native proteins, suggesting that the fibrils are well-packed.

Keywords: amyloid fibril; X-ray diffraction; insulin; diamond anvil cell; elastic modulus

1. Introduction

Amyloid fibrils are commonly associated with neurodegenerative diseases, of which Alzheimer's and Parkinson's diseases are the most prominent. In 1999, however, Dobson and co-workers made a chance observation, which eventually led to the hypothesis that the formation of amyloid fibrils is inherent to the polypeptide backbone [1]. Ever since, there has been a growing number of scientists involved in the study of the biophysics of amyloid fibril self-assembly and the possible use of amyloid fibrils, for instance as scaffolds, in nanotechnology, in addition to the investigation of the medical aspects of their occurrence [2,3]. Recent analyses of the mechanical properties of amyloid fibrils from various polypeptides using atomic force microscopy (AFM) revealed that they possess high strength and stiffness [4,5]. This further emphasizes their potential use in nanotechnology.

Hydrostatic pressure, which influences hydrogen bonds (HBs) and the hydrophobic effect, can be used to perturb biological systems to study protein folding, misfolding or denaturation events [6]. This provides information on the volume changes associated with each process, and

*Corresponding author. Email: filip.meersman@chem.kuleuven.be

ISSN 0895-7959 print/ISSN 1477-2299 online

DOI: 10.1080/08957950903350975
http://www.informaworld.com

the compressibility associated with a particular state. The important thermodynamic quantities can be interpreted in terms of the degree of hydration and presence of cavities, and overall volume fluctuations, respectively. In the particular case of amyloid fibrils, this yields information about the non-covalent intermolecular interactions involved in the fibril formation process, as well as about the packing of the fibrils [7,8]. An important recent finding is that amyloid fibrils undergo a maturation process, indicative of a certain conformational plasticity of the early fibrils [9]. The study of the time dependence of fibril stability revealed an optimization of the packing and the increasingly important role of HBs as self-assembly proceeds.

Here, we present preliminary work on the use of synchrotron X-ray diffraction in a diamond anvil cell (DAC) to probe the compressibility of amyloid fibrils in aqueous solution, and the derivation of their mechanical properties from the compression data by the application of equations of state (EOS). Our approach provides an alternative to AFM studies to derive the mechanical properties of amyloid fibrils. Insulin fibrils are used as a model system, as these have been shown to resist pressures up to 1.0 GPa by FTIR spectroscopy [10].

2. Experimental

Insulin amyloid fibrils were prepared as described previously [10]. Briefly, insulin (Sigma, Bornem, Belgium) was dissolved in water at 20 mg mL^{-1} and the pH was adjusted to ~2 using diluted HCl. The solution was subsequently left at 70°C for several hours. Under these conditions, amyloid fibrils grow and further self-assemble into spherulites [11]. The nature of the sample was verified by optical microscopy (Figure 1) and FTIR spectroscopy (data not shown).

For *in situ* high-pressure X-ray diffraction measurements, the mature amyloid samples were loaded into a cylindrical DAC. The sample was contained within a 200 μm hole drilled in a Re gasket. Ruby chips were added for pressure determination. X-ray diffraction studies were performed at the Swiss-Norwegian Beamline (European Synchrotron Radiation Facility). Here, the wavelength was set to 0.07183 nm. The sample-to-detector distance and the image plate inclination angles were calibrated using a crystalline LaB_6 standard.

The two-dimensional diffraction images were azimuthally integrated using the Fit2D program (V12.034) [12], yielding one-dimensional intensity $I(s)$ versus s ($s = d^{-1} = 2\sin\theta/\lambda$, where 2θ is the diffraction angle and λ the wavelength). The peak maximum was determined by peak fitting using PeakFit V. 4 software (Systat Software Inc).

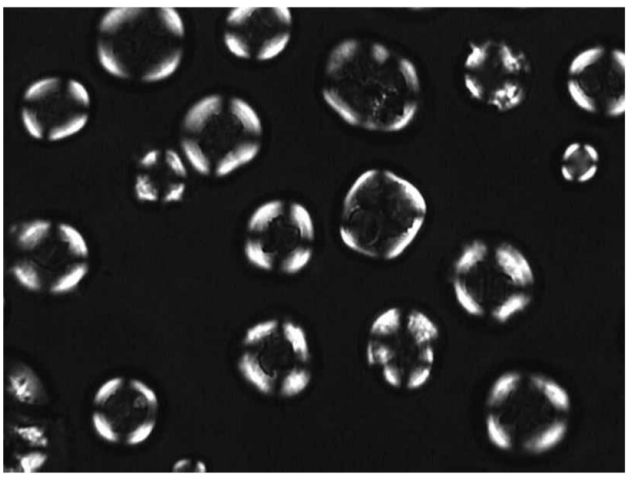

Figure 1. Characterization of insulin spherulites under cross-polarized light. The appearance of the Maltese cross indicates the radial distribution of the amyloid fibrils.

3. Results and discussion

Diffraction patterns of aligned amyloid fibrils generally have two main reflections, indicative of the underlying cross-β structure: a sharp meridional reflection at 4.7 Å and a diffuse equatorial reflection at 8–12 Å [13]. These reflections correspond to the strand–strand and inter-sheet distances, respectively. No alignment procedures were applied in our studies so that the observed patterns represent an isotropic average of the fibril orientations in their aqueous solution. The 8–12 Å reflection cannot be observed. A recent study of three fragments of the yeast prion Sup35 also found that the 10 Å reflection is absent in the hydrated state [14]. The 10 Å reflection was therefore considered to be an artefact associated with the use of dried fibril samples. The equatorial reflection has, however, been observed for unaligned fibrils from lysozyme and the transthyretin peptide 105-115 in concentrated solutions [13]. One possible explanation for this apparent contradiction is that the high dispersion of amyloid fibrils in solution may result in lower order, broadening the inter-sheet reflection, thereby reducing its average intensity below the noise level of the pattern [15].

We used the intense meridional reflection at ~4.7 Å to probe changes in fibril structure as a function of pressure in the range 0.0001–10 GPa (Figure 2). Note that liquid water transforms into ice VI above 1.4 GPa and into ice VII at pressures above 2.1 GPa. The crystallization of the water results in a drop of the pressure due to the smaller volume of the ice polymorphs. However, the crystallization has no apparent effect on the amyloid fibrils and did not interfere with our analysis. As pressure is increased, the diffraction peak shifts to smaller distances, indicating a shortening of the inter-strand distance along the fibril axis (Figure 2). Such a change also results in a decrease in the HB distance between adjacent β-sheets aligned normal to the fiber axis. It is known that HBs in protein structures can either shorten or lengthen under compression [16], and both red- and blue-shifts have been observed for characteristic IR peaks associated with H-bonding in fibril samples [9]. The increased width of the diffraction peak under compression is indicative of a pressure-induced heterogeneity in the HB distance, reflecting local differences in compressibility. All changes were found to be reversible upon decompression.

The pressure-dependence of the normalized inter-strand distance (d/d_o) was analyzed using the one-dimensional analog of the Murnaghan EOS (Equation (1)) and the Vinet EOS (Equation (2)), both of which have been used successfully to study the compressional behavior of materials in

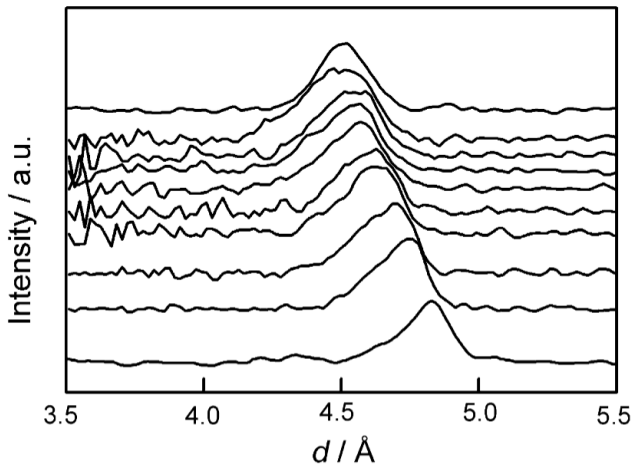

Figure 2. Baseline-corrected X-ray diffraction patterns of insulin amyloid fibrils.

the low-pressure regime (Figure 3) [17,18]:

$$\frac{d}{d_o} = \left[1 + \left(\frac{Y_o'}{Y_o}\right) p\right]^{-1/Y_o'}, \tag{1}$$

$$p = 3Y_o(1-x)x^{-2} \cdot \exp\left[\frac{3}{2}(Y_o' - 1)(1-x)\right]. \tag{2}$$

Here Y_o is the elastic modulus and Y_o' its pressure derivative; p is the pressure in GPa and $x = (d/d_o)^{1/3}$. By defining a function $H = px^2/[3(1-x)]$, the Vinet EOS can be linearized (Equation (3)) [18]:

$$\ln H = \ln Y_o + \left[\frac{3}{2}(Y_o' - 1)(1-x)\right]. \tag{3}$$

This is shown in Figure 3 (inset), where Y_o is given by the slope of the curve and the intercept is equal to $\ln Y_o'$. The linearity of the plot rules out the occurrence of a phase transition in the system. The results of these fittings are given in Table 1, and indicate that the elastic moduli obtained by the different EOS are in good agreement. Our Y_o values are larger than those deduced from AFM measurements [4,5]. An important advantage of our methodology compared with the AFM approach is that we directly probe the compressibility of the cross-β structure along the fibril's longitudinal axis, rather than exerting a force perpendicular to the axis with a cantilever [4]. The AFM methodology also involves numerous assumptions that are not evident in biological materials [19]. Moreover, our method determines the compression independent of the higher order hierarchy of the assembly, whereas in AFM this will give different results. For instance, Guo and Akhremitchev [20] determined values ranging from 5 to 50 MPa for the elastic modulus of insulin fibrils, whereas Smith et al. [4] reported an elastic (Young's) modulus of 3–6 GPa for a two-filament fibril. Most likely the interaction between the protofilaments was measured in the

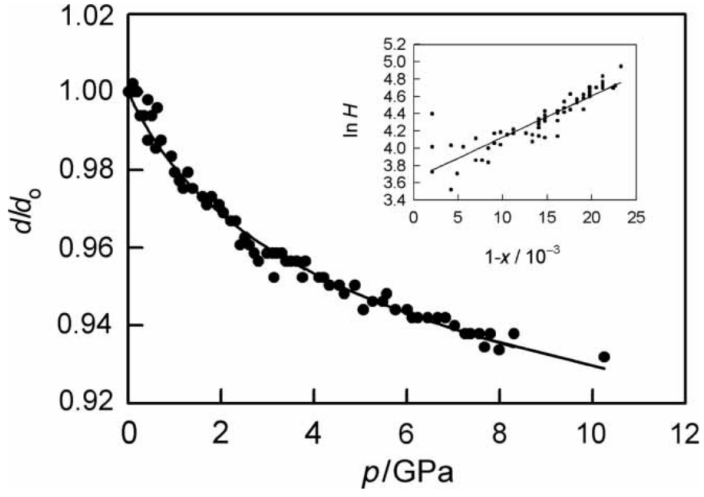

Figure 3. Pressure-dependence of the inter-strand spacing in insulin amyloid fibrils. The full line is the first-order Murnaghan EOS fit to the data. The inset shows a linearized representation of the data and the corresponding fit to the linearized Vinet EOS.

Table 1. Elastic modulus (Y_o) and its pressure derivative (Y_o') of insulin amyloid fibrils.

Equation of state	Y_o (GPa)	Y_o'
One-dimensional Murnaghan	37.3 ± 1.9	30.2 ± 1.6
Linearized Vinet	38.4 ± 1.9	32.9 ± 2.2

former case. We note that our directly determined elastic moduli are in good agreement with the predicted values using simplified models for inter-strand H-bonding and repulsive interactions along the fibril axis [5].

The isothermal linear compressibility $\beta(\beta = 1/Y_o)$ is $0.027\,\mathrm{GPa}^{-1}$. The corresponding HB shortening is -0.078 Å/GPa. For comparison, the average HB shortening in a native protein is $-0.1\,\text{Å}\,\mathrm{GPa}^{-1}$, and $-0.09\,\text{Å}\,\mathrm{GPa}^{-1}$ in ice-Ih [16,21,22]. These values indicate that the mature fibrils must be well-packed with little void space between the β-sheets, similar to native proteins and molecular crystals. This is corroborated by the fact that the typical cross-β structure spacing at ∼4.8 Å is still observed at the highest pressure attained in these studies (10.3 GPa), implying that the fibrils do not dissociate at these high pressures, since pressure treatment favors those structures occupying the smallest volume [7,23].

Although the local and long-range forces that maintain the amyloid fibril structure are the same as those involved in native proteins, the globular forms have relatively low thermodynamic stability, especially at high pressure [7]. This difference can be traced to the more efficient packing geometry of the polypeptide subunits that also results in the lowered compressibility of fibrillar structures. Optimizing the packing geometry will enable further stabilizing interactions such as HBs or the stacking of aromatic groups to come into play. The need for efficient packing and optimizing non-covalent interactions has already been shown to steer the early stages of the amyloid fibril formation process [24].

In summary, we have presented a novel approach that allows a direct estimation of the compression of the cross-β structure along the fiber axis. In addition, our results emphasize the importance of packing in addition to the recently highlighted role of HBs [5].

Acknowledgements

We thank Swiss-Norwegian Beamline at ESRF for access to the beamline. F.M. is a postdoctoral research fellow of the Research Foundation Flanders (FWO-Vlaanderen). R.Q.C. and P.F.M. are supported by EPSRC Portfolio grant EP/D504872 (to P.F.M., C.R.A. Catlow and P. Barnes) and EPSRC Senior Research Fellowship EP/D07357X (PFM).

References

[1] F. Chiti and C.M. Dobson, *Protein misfolding, functional amyloid and human disease*, Annu. Rev. Biochem. 75 (2006), pp. 333–366.
[2] T. Scheibel, R. Parthasarathy, G. Sawicki, X.-M. Lin, H. Jaeger, and S.L. Lindquist, *Conducting nanowires built by controlled self-assembly of amyloid fibers and selective metal deposition*, Proc. Natl. Acad. Sci. USA 100 (2003), pp. 4527–4532.
[3] A.J. Baldwin, R. Bader, J. Christodoulou, C.E. MacPhee, C.M. Dobson, and P.D. Barker, *Cytochrome display on amyloid fibrils*, J. Am. Chem. Soc. 128 (2006), pp. 2162–2163.
[4] J.F. Smith, T.P.J. Knowles, C.M. Dobson, C.E. MacPhee, and M.E. Welland, *Characterization of the nanoscale properties of individual amyloid fibrils*, Proc. Natl. Acad. Sci. USA 103 (2006), pp. 15806–15811.
[5] T.P. Knowles, A.W. Fitzpatrick, S. Meehan, H.R. Mott, M. Vendruscolo, C.M. Dobson, and M.E. Welland, *Role of intermolecular forces in defining material properties of protein nanofibrils*, Science 318 (2007), pp. 1900–1903.
[6] F. Meersman, C.M. Dobson, and K. Heremans, *Protein unfolding, amyloid fibril formation and configurational energy landscapes under high pressure conditions*, Chem. Soc. Rev. 35 (2006), pp. 908–917.
[7] F. Meersman and C.M. Dobson, *Probing the pressure-temperature stability of amyloid fibrils provides new insights into their molecular properties*, Biochim. Biophys. Acta 1764 (2006), pp. 452–460.
[8] K. Akasaka, A.R. Latif, A. Nakamura, K. Matsuo, H. Tachibana, and K. Gekko, *Amyloid protofibril is highly voluminous and compressible*, Biochemistry 46 (2007), pp. 10444–10450.
[9] C. Dirix, F. Meersman, C.E. MacPhee, C.M. Dobson, and K. Heremans, *High hydrostatic pressure dissociates early aggregates of TTR105-115, but not the mature amyloid fibrils*, J. Mol. Biol. 347 (2005), pp. 903–909.
[10] S. Grudzielanek, V. Smirnovas, and R. Winter, *Solvation-assisted pressure tuning of insulin fibrillation: From novel aggregation pathways to biotechnological applications*, J. Mol. Biol. 356 (2006), pp. 497–509.
[11] M.R.H. Krebs, C.E. MacPhee, A.F Miller, I.E. Dunlop, C.M. Dobson, and A.M. Donald, *The formation of spherulites by amyloid fibrils of bovine insulin*, Proc. Natl. Acad. Sci. USA 101 (2004), pp. 14420–14424.
[12] A.P. Hammersley, S.O. Svensson, M. Hanfland, A.N. Fitch, and D. Häusermann, *Two-dimensional detector software: From real detector to idealised image or two-theta scan*, High Press. Res. 14 (1996), pp. 235–248.

[13] A.M. Squires, G.L. Devlin, S.L. Gras, A.K. Tickler, C.E. MacPhee, and C.M. Dobson, *X-ray scattering study of the effect of hydration on the cross-β structure of amyloid fibrils*, J. Am. Chem. Soc. 128 (2006), pp. 11738–11739.
[14] K. Kishimoto, H. Hasegawa, H. Suzuki, K. Taguchi, K. Namba, and M. Yoshida, *β-helix is a likely core structure of yeast prion Sup35 amyloid fibers*, Biochem. Biophys. Res. Commun. 315 (2004), pp. 739–745.
[15] O.S. Makin and L.C. Serpell, *Structures for amyloid fibrils*, FEBS J. 272 (2005), pp. 5950–5961.
[16] N. Colloc'h, E. Girard, A.C. Dhaussy, R. Kahn, I. Ascone, M. Mezouar, and R. Fourme, *High pressure macromolecular crystallography: The 140-MPa crystal structure at 2.3 Å resolution of urate oxidase, a 135-kDa tetrameric assembly*, Biochim. Biophys. Acta 1764 (2006), pp. 391–397.
[17] M. Hanfland, H. Besiter, and K. Syassen, *Graphite under pressure: Equation of state and first-order Raman modes*, Phys. Rev. B 39 (1989), pp. 12598–12603.
[18] P. Vinet, J. Ferrante, J.H. Rose, and J.R. Smith, *Compressibility of solids*, J. Geophys. Res. 92 (1987), pp. 9319–9325.
[19] A. Vinckier and G. Semenza, *Measuring elasticity of biological materials by atomic force microscopy*, FEBS Lett. 430 (1998), pp. 12–16.
[20] S. Guo and B.B. Akhremitchev, *Packing density and structural heterogeneity of insulin amyloid fibrils measured by AFM nanoindentation*, Biomacromolecules 7 (2006), pp. 1630–1636.
[21] M.P. Williamson, K. Akasaka, and M. Refaee, *The solution structure of bovine pancreatic trypsin inhibitor at high pressure*, Protein Sci. 12 (2003), pp. 1971–1979.
[22] T.C. Sivakumar, H.A.M. Chew, and G.P. Johari, *Effect of pressure on the Raman spectrum of ice*, Nature 275 (1978), pp. 524–525.
[23] J.L. Silva, D. Foguel, and C. Royer, *Pressure provides new insights into protein folding, dynamics and structure*, Trends Biochem. Sci. 26 (2001), pp. 612–618.
[24] J. Gsponer, U. Habertür, and A. Caflisch, *The role of side-chain interactions in the early steps of aggregation: Molecular dynamics simulations of an amyloid-forming peptide from the yeast prion Sup35*, Proc. Natl. Acad. Sci. USA 100 (2003), pp. 5154–5159.